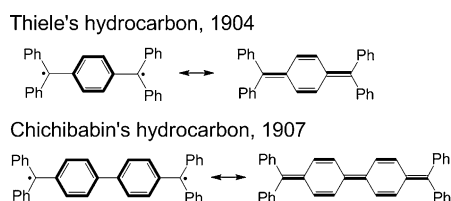


Nitrogen Analogues of Thiele's Hydrocarbon**

Yuanting Su, Xingyong Wang, Yuantao Li, You Song, Yunxia Sui, and Xinping Wang*

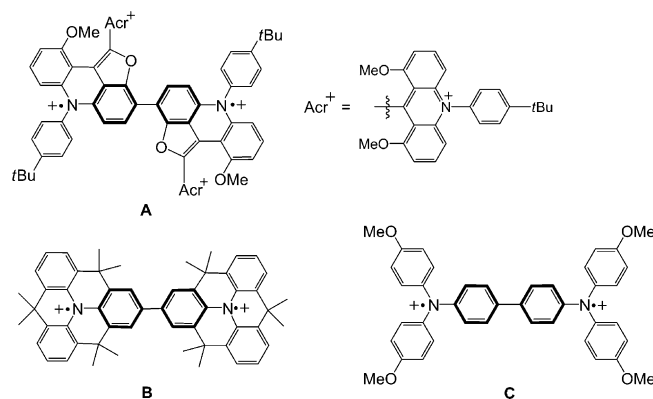
Abstract: A series of bis[*N,N*-di-(4-methoxyphenyl)amino]arene dications **1**²⁺–**3**²⁺ have been synthesized and characterized. Their electronic structures were investigated by various experiments assisted by theoretical calculations. It was found that they are singlets in the ground state and that their diradical character is dependent on the bridging moiety. **3**²⁺ has a smaller singlet–triplet energy gap and its excited triplet state is thermally readily accessible. The work provides a nitrogen analogue of Thiele's hydrocarbon with considerable diradical character.

St able diradicaloids delocalized over π -conjugated systems have attracted much attention due to their unique chemical bonding, interesting physical properties (optical, electronic, magnetic, etc.), and promising applications as functional materials in molecular electronics.^[1] Thiele's and Chichibabin's hydrocarbons (Scheme 1),^[2] which were prepared

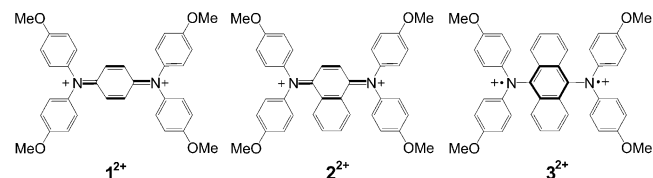


Scheme 1. Thiele's and Chichibabin's hydrocarbons.

shortly after Gomberg's synthesis of the triphenylmethyl radical,^[3] have been the subjects of interest for more than one century. Both possess a characteristic resonance structure between an open-shell diradical and a closed-shell quinonoid



Scheme 2. Nitrogen analogues of Chichibabin's hydrocarbons.



Scheme 3. Bis[*N,N*-di-(4-methoxyphenyl)amino]arene dications.

form. Their isolable derivatives and analogues with enhanced stability and diradical character have also been explored.^[1,4] Very recently Kamada et al. and our group reported stable nitrogen analogues of Chichibabin's hydrocarbon as diradicaloids (**A–C** in Scheme 2).^[5] Herein we present the isolation and characterization of nitrogen analogues of Thiele's hydrocarbon (**1**²⁺–**3**²⁺ in Scheme 3).

Neutral **1–3** were synthesized under standard Buchwald–Hartwig Pd-catalyzed amination of aryl halides by literature procedures.^[6] Upon oxidation with Ag[Al(OR_F)₄] (2 equiv, OR_F = OC(CF₃)₃)^[7–9] in CH₂Cl₂, the neutral precursors **1–3** were converted to dications **1**²⁺–**3**²⁺ in high yields, respectively. The resulting dication salts are thermally stable as crystals under air and can be stored for several days at room temperature. The electronic and geometric structures of these dications were systematically investigated by UV/Vis, electron paramagnetic resonance (EPR), single-crystal X-ray diffraction, and superconducting quantum interference device (SQUID) measurements, in conjunction with DFT computations.

Crystals suitable for X-ray crystallographic studies were obtained by cooling solutions of salts **2**²⁺·2[Al(OR_F)₄][–] and **3**²⁺·2[Al(OR_F)₄][–] in CH₂Cl₂,^[10] however, attempts to grow crystals of **1**²⁺·2[Al(OR_F)₄][–] failed. The structures of the dications **2**²⁺ and **3**²⁺ are illustrated as stereoviews in Figure 1 with structural parameters, some of which are given in

[*] Y. Su,^[†] Dr. X. Wang,^[†] Y. Li, Prof. Y. Song, Prof. X. Wang
State Key Laboratory of Coordination Chemistry
School of Chemistry and Chemical Engineering
Collaborative Innovation Center of Advanced Microstructures
Nanjing University, Nanjing 210093 (China)
E-mail: xpwang@nju.edu.cn

Y. Sui

Centre of Modern Analysis, Nanjing University
Nanjing 210093 (China)

[†] These authors contributed equally to this work.

[**] We thank the National Natural Science Foundation of China (Grants 91122019, 21171087), the Major State Basic Research Development Program (2013CB922101), the Natural Science Foundation of Jiangsu Province (Grant BK20140014), and 2014 Jiangsu Province Innovation for Ph.D Candidate (KYZZ-0026, Y.S.) for financial support. We also thank Dr. Zaichao Zhang and Dr. Yue Zhao for assistance on crystallographic work, and Dr. Tianwei Wang for the SQUID measurements.

Supporting information for this article is available on the WWW under <http://dx.doi.org/10.1002/anie.201410256>.

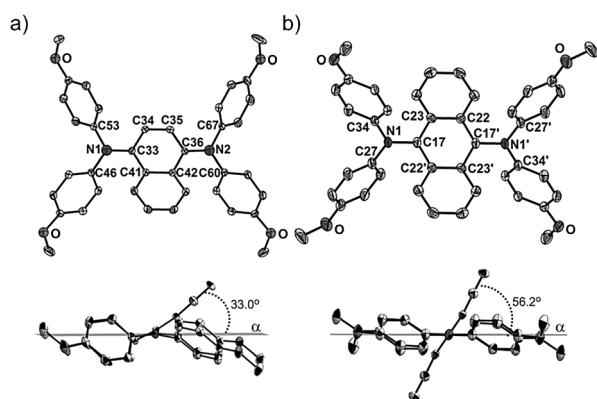
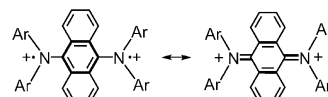


Figure 1. Thermal ellipsoid (50%) drawings of a) 2^{2+} and b) 3^{2+} : top views (upper) and side views (lower). Hydrogen atoms were omitted for clarity. Selected bond lengths (Å) and angles (deg): in 2^{2+} , N1–C33 1.354(3), N1–C46 1.439(3), N1–C53 1.423(3), N2–C36 1.355(3), N2–C60 1.431(3), N2–C67 1.431(3), C33–C34 1.421(3), C34–C35 1.356(3), C35–C36 1.428(3), C36–C42 1.462(3), C41–C42 1.430(3), C33–C41 1.461(3), C33–N1–C46 123.91(18), C33–N1–C53 120.05(18), C46–N1–C53 115.79(17), C36–N2–C60 124.11(18), C36–N2–C67 120.27(18), C60–N2–C67 115.48(17); in 3^{2+} , N1–C17 1.405(4), N1–C27 1.409(4), N1–C34 1.409(5), C17–C23 1.431(5), C22–C23 1.432(5), C17–C22 1.430(5), C17–N1–C27 120.1(3), C17–N1–C34 119.8(3), C27–N1–C34 120.1(3).

Table S2 in the Supporting Information (SI). Two nitrogen atoms are nearly coplanar (α) with six neighboring carbon atoms in both dications 2^{2+} and 3^{2+} . The plane (α) more largely deviates (56.2°) from the anthracene moiety in 3^{2+} than naphthalene (33.0°) in 2^{2+} due to the steric repulsion. In 2^{2+} the average N–C bond length (1.354(3) Å) to the naphthalene moiety is much shorter than that (1.409(4) Å) to the peripheral aryl ring systems (N–Ar), which, together with the short C34–C35 bond (1.356(3) Å), shows a quasi-quinoidal^[11] and closed-shell ground-state structure for 2^{2+} . In contrast, in 3^{2+} the average N–C bond length (1.405(4) Å) to the anthracene moiety is close to that (1.430(5) Å) to the peripheral aryl ring systems (N–Ar), and significantly longer than that (1.354(3) Å) in 2^{2+} , indicating that 3^{2+} may have a diradical character.

To further understand the electronic structures, we performed calculations for species 1^{2+} – 3^{2+} .^[12] Full geometry optimizations were performed at the (U)B3LYP/6-31G(d) level and the obtained stationary points were characterized by frequency calculations. The calculated energy differences $\Delta E_{\text{OS-CS}}$ between the open-shell (OS) singlet diradicals and closed-shell (CS) singlet states increase, whereas the singlet–triplet energy gaps $\Delta E_{\text{OS-T}}$ decrease from 1^{2+} to 3^{2+} , showing a clear bridging dependence (Table S2, SI).^[13] The N–C and C–C bond lengths in the X-ray crystal structure of 2^{2+} are close to those of the closed-shell singlet, whereas the bond lengths of 3^{2+} are found to be between those for the optimized closed-shell singlet and diradical triplet, indicating a singlet ground state with an intermediate diradical character for 3^{2+} . Dication 3^{2+} is thus best described as a resonance hybrid of diradical structure and quinoidal structure (Scheme 4), similar to Thiele’s hydrocarbon (Scheme 1). However, the value of diradical character y calculated at the UBHandHLYP/6-31G(d) level, which is estimated by the occupancy of the



Scheme 4. Resonance structures of 3^{2+} .

lowest unoccupied natural orbital (LUNO) to represent the “degree” of the singlet diradical character,^[14] of the X-ray structure of 3^{2+} (0.63) is much higher than that (0.18)^[15] of Thiele’s hydrocarbon. The HOMO(α) and LUMO(α) orbitals of 3^{2+} -OS are delocalized over one amine unit, with larger coefficients from the peripheral aryl rings (Figure 2 a,b). The spin density is distributed through the whole molecule in 3^{2+} -OS (Figure 2c).

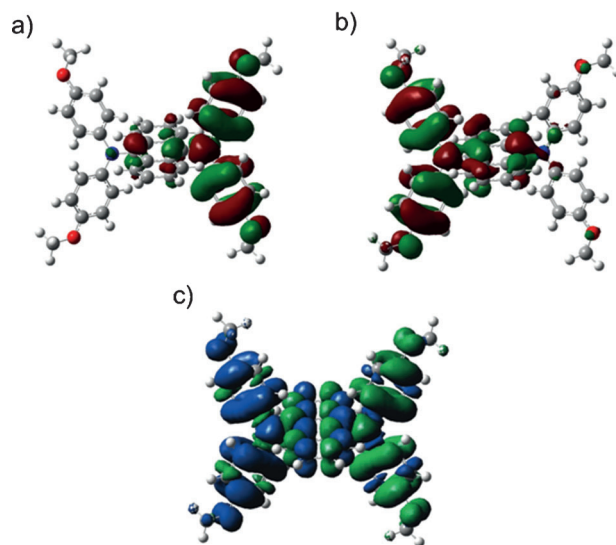


Figure 2. a) LUMO (α), b) HOMO (α), and c) spin densities of 3^{2+} -OS, calculated at the UB3LYP/6-31G(d) level.

The diradical character of 3^{2+} is consistent with its maximum absorption of the lowest energy transition in the near-infrared region (982 nm, Figure 3), which is greatly blue-shifted to 822 nm for 1^{2+} and 842 nm for 2^{2+} . Time-dependent (TD) DFT^[12b] calculation at the UPBE0/6-31G(d) level on the open-shell singlet geometry of 3^{2+} indicates the maximum absorption is due to HOMO→LUMO and HOMO-1→

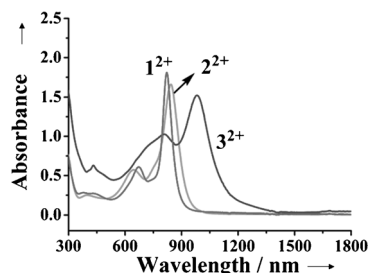


Figure 3. Absorption spectra of 1×10^{-4} M 1^{2+} , 2^{2+} , and 3^{2+} in CH_2Cl_2 at 25°C .

LUMO transitions, and in reasonable agreement with the experimental absorption (Figure S3, SI). The small HOMO–LUMO gap is a typical indication for a significant diradical character.

The magnetic properties of $\mathbf{1}^{2+}$ – $\mathbf{3}^{2+}$ were examined by EPR and SQUID measurements. $\mathbf{1}^{2+}$ and $\mathbf{2}^{2+}$ in solution and the solid state showed no EPR signal, indicating they have closed-shell structures in the ground state. The solution of $\mathbf{3}^{2+}$ was also EPR-silent, which may be due to the low spin concentration in the dilute solution. The powder EPR spectrum (Figure 4a) of $\mathbf{3}^{2+}\cdot 2[\text{Al}(\text{OR}_F)_4]^-$, however, is typical for a triplet state. The observed $\Delta m_s = \pm 2$ transition further indicates that $\mathbf{3}^{2+}$ is a diradical dication upon thermal activation. The zero-field parameters were determined by spectral simulation as $D = 13.4$ mT (12.5×10^{-3} cm $^{-1}$) and $E = 1.28$ mT (1.19×10^{-3} cm $^{-1}$), with an anisotropic g factor ($g_x = 2.0050$, $g_y = 2.0045$, $g_z = 2.0053$). The hyperfine coupling constant with N atoms is $A_{xx}(\text{N}) = 0$, $A_{yy}(\text{N}) = 0.98$, and $A_{zz}(\text{N}) = 0$ mT, respectively. The average spin–spin distance from D was estimated to be 5.9 Å, which is slightly longer than the distance (5.6 Å) between the two N atoms in the X-ray structure, indicating that the two unpaired electrons are not only residing on two nitrogen atoms, but to some extent delocalized on the bridging anthracene unit and the peripheral aryl rings. Correspondingly the SQUID measurements on $\mathbf{1}^{2+}$ and $\mathbf{2}^{2+}$ only showed diamagnetism (Figures S1 and S2, SI), consistent with their closed-shell singlet ground states. In contrast, an increasing susceptibility above 100 K was observed for the powder sample of $\mathbf{3}^{2+}$ (Figure 4b). Careful fitting with the Bleaney–Bowers equation^[16] and Hamiltonian $\mathcal{H} = -2J \mathbf{S}_1 \mathbf{S}_2$ ($S_1 = S_2 = 1/2$) gave a small singlet–triplet

energy gap ($\Delta E_{S-T} = -1.4$ kcal mol $^{-1}$), which agrees well with the calculated value (-1.47 kcal mol $^{-1}$) at the UB3LYP/6-31G(d) level.^[17]

Seemingly the steric repulsion arising from the central bridge with the peripheral aryls plays an important role in the diradical character of $\mathbf{3}^{2+}$. To investigate the correlation between the degree of geometric twisting and increased diradical character, a series of Thiele's nitrogen analogues in which the bridge part was modified with methyl groups were theoretically studied (Table S3, SI). Correlations between the degree of geometric twisting and increased diradical character are shown in Figure S4,5 in the SI, which clearly show that a gradual replacement of the hydrogen atoms of the central bridge moiety by methyl groups leads to increased steric repulsion, stronger geometric twisting, and increased diradical character. In addition, the enhanced diradical character may also be attributed to the recovery of aromaticity of bridging aryl rings. The determination of nucleus-independent chemical shift (NICS) values suggests a quinoid character of the bridging benzene rings for $\mathbf{1}^{2+}$ and $\mathbf{2}^{2+}$, whereas a more benzenoid character is suggested for $\mathbf{3}^{2+}$ (Figure S6, SI), which is consistent with experimental observations.

In summary, we have synthesized and characterized a series of bis[*N,N*-di-(4-methoxyphenyl)amino]arene dications $\mathbf{1}^{2+}$ – $\mathbf{3}^{2+}$. The work demonstrated an interesting bridging dependence of the structures, energy gaps, diradical character, and spectroscopic as well as magnetic properties. The steric repulsion and recovery of aromaticity of bridging aryl rings causes a smaller singlet–triplet energy gap for $\mathbf{3}^{2+}$ and its excited triplet state is thermally readily accessible. The work provides a nitrogen analogue of Thiele's hydrocarbon with considerable diradical character. Its application in molecular electronics is worth further investigation.

Experimental Section

General Procedures: All manipulations were performed under an Ar or N₂ atmosphere by using standard Schlenk or glove box techniques. Solvents were dried prior to use. Bis[*N,N*-di-(4-methoxyphenyl)amino]arenes (**1**, **2**, and **3**)^[6] and Ag[Al(OR_F)₄]^[7] were prepared by the published procedures. EPR spectra were obtained using a Bruker EMX-10/12 variable-temperature apparatus. Magnetic measurements were performed using a Quantum Design MPMS XL-7 SQUID magnetometer in the temperature range 5–350 K with a field up to 7 T. UV/Vis spectra were recorded on the Lambda 750 spectrometer. Element analyses were performed at Shanghai Institute of Organic Chemistry, the Chinese Academy of Sciences. X-ray crystal structures were obtained by using Bruker APEX DUO CCD detector.

Syntheses of dication salts: Under anaerobic and anhydrous conditions, a mixture of bis[*N,N*-di-(4-methoxyphenyl)amino]arene and Ag[Al(OR_F)₄] in CH₂Cl₂ (≈ 50 mL) was stirred at room temperature overnight. The resultant solution was filtered to remove the gray precipitate (Ag metal). The filtrate was then concentrated and stored at around -30°C for 1 day to afford crystals or powder.

$\mathbf{1}^{2+}\cdot 2[\text{Al}(\text{OR}_F)_4]^-$: **1** (0.1065 g, 0.200 mmol) and Ag[Al(OR_F)₄] (0.4514 g, 0.420 mmol); blue powder. Yield: 0.3182 g, 64.5 %; UV/Vis (CH₂Cl₂): $\lambda_{\text{max}} = 822$ and 672 nm; elemental analysis (%) calcd: C 32.13, H 1.31, N 1.14; found: C 31.34, H 1.31, N 0.99.

$\mathbf{2}^{2+}\cdot 2[\text{Al}(\text{OR}_F)_4]^-$: **2** (0.1748 g, 0.300 mmol) and Ag[Al(OR_F)₄] (0.6663 g, 0.620 mmol); deep-blue crystals. Yield: 0.5842 g, 77.4 %; UV/Vis (CH₂Cl₂): $\lambda_{\text{max}} = 842$ and 645 nm; elemental analysis (%) calcd: C 33.40, H 1.36, N 1.11.; found: C 33.40, H 1.35, N 1.14.

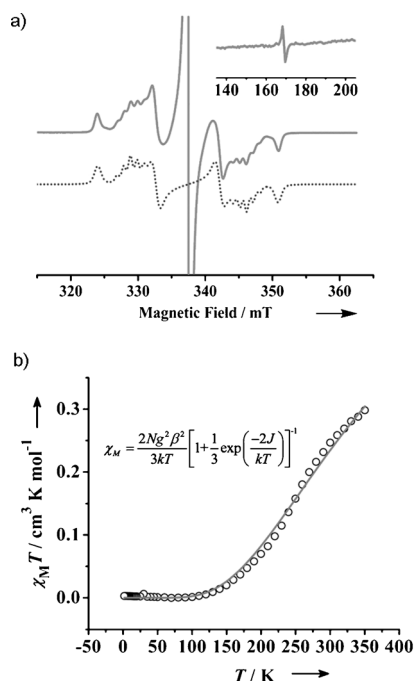


Figure 4. a) The powder EPR spectrum of $\mathbf{3}^{2+}$ at 110 K. The solid and dotted lines indicate observed and simulated spectra, respectively. The central peak shows the signal derived from the monoradical impurity; and b) $\chi_M T$ versus T curve in the SQUID measurements for the powder of $\mathbf{3}^{2+}$ and the fitting plot obtained with the Bleaney–Bowers equation.

$3^{2+} \cdot 2[\text{Al}(\text{OR}_F)_4]^-$: **3** (0.1266 g, 0.200 mmol) and $\text{Ag}[\text{Al}(\text{OR}_F)_4]$ (0.4729 g, 0.440 mmol); blue-green crystals. Yield: 0.3553 g, 69.2%; UV/Vis (CH_2Cl_2): $\lambda_{\text{max}} = 982$ and 808 nm; elemental analysis (%) calcd: C 34.62, H 1.41, N 1.09; found: C 34.61, H 1.40, N 1.24.

Received: October 19, 2014

Published online: December 11, 2014

Keywords: diradicals · EPR spectroscopy · singlet state · triplet state · X-ray structure

- [1] a) M. Abe, J. Ye, M. Mishima, *Chem. Soc. Rev.* **2012**, *41*, 3808; b) Z. Sun, Q. Ye, C. Chi, J. Wu, *Chem. Soc. Rev.* **2012**, *41*, 7857; c) J. Casado, R. P. Ortiz, J. T. L. Navarrete, *Chem. Soc. Rev.* **2012**, *41*, 5672; d) M. Abe, *Chem. Rev.* **2013**, *113*, 7011; e) M. Nakano, R. Kishi, S. Ohta, H. Takahashi, T. Kubo, K. Kamada, K. Ohta, E. Botek, B. Champagne, *Phys. Rev. Lett.* **2007**, *99*, 033001.
- [2] a) J. Thiele, H. Balhorn, *Chem. Ber.* **1904**, *37*, 1463; b) A. E. Chichibabin, *Chem. Ber.* **1907**, *40*, 1810; c) L. K. Montgomery, J. C. Huffman, E. A. Jurczak, M. P. Grendze, *J. Am. Chem. Soc.* **1986**, *108*, 6004, and references therein; d) The simplest nitrogen analogue of Thiele's hydrocarbon, that is, *p*-phenylenediamine dications, have been theoretically studied. M. De Wergifosse, F. Wautelet, B. Champagne, R. Kishhi, K. Fukuda, H. Matsui, M. Nakano, *J. Phys. Chem. A* **2013**, *117*, 4709.
- [3] a) M. Gomberg, *J. Am. Chem. Soc.* **1900**, *22*, 757; b) M. Gomberg, *Chem. Ber.* **1900**, *33*, 3150.
- [4] Selected examples: a) W. W. Porter III, T. P. Vaid, A. L. Rheingold, *J. Am. Chem. Soc.* **2005**, *127*, 16559; b) A. Kikuchi, F. Iwahori, J. Abe, *J. Am. Chem. Soc.* **2004**, *126*, 6526; c) S. F. Nelsen, R. F. Ismagilov, Y. Teki, *J. Am. Chem. Soc.* **1998**, *120*, 2200; d) T. Nozawa, M. Nagata, M. Ichinohe, A. Sekiguchi, *J. Am. Chem. Soc.* **2011**, *133*, 5773; e) Z. Zeng, M. Ishida, J. L. Zafra, X. Zhu, Y. M. Sung, N. Bao, R. D. Webster, B. S. Lee, R. Li, W. Zeng, Y. Li, C. Chi, J. T. L. Navarrete, J. Ding, J. Casado, D. Kim, J. Wu, *J. Am. Chem. Soc.* **2013**, *135*, 6363; f) K. Okada, T. Imakura, M. Oda, H. Murai, M. Baumgarten, *J. Am. Chem. Soc.* **1996**, *118*, 3047.
- [5] a) K. Kamada, S. Fuku-en, S. Minamide, K. Ohta, R. Kishi, M. Nakano, H. Matsuzaki, H. Okamoto, H. Higashikawa, K. Inoue, S. Kojima, Y. Yamamoto, *J. Am. Chem. Soc.* **2013**, *135*, 232; b) X. Zheng, X. Wang, Y. Qiu, Y. Li, C. Zhou, Y. Sui, Y. Li, J. Ma, X. Wang, *J. Am. Chem. Soc.* **2013**, *135*, 14912; c) Y. Su, X. Wang, X. Zheng, Z. Zhang, Y. Song, Y. Sui, Y. Li, X. Wang, *Angew. Chem. Int. Ed.* **2014**, *53*, 2857; *Angew. Chem.* **2014**, *126*, 2901.
- [6] a) C. Lambert, G. Nöll, *J. Am. Chem. Soc.* **1999**, *121*, 8434; b) C. Lambert, C. Risko, V. Coropceanu, J. Schelter, S. Amthor, N. E. Gruhn, J. C. Durivage, J. L. Brédas, *J. Am. Chem. Soc.* **2005**, *127*, 8508.
- [7] I. Krossing, *Chem. Eur. J.* **2001**, *7*, 490.
- [8] Reviews on weakly coordinating anions: a) I. Krossing in *Comprehensive Inorganic Chemistry II: From Elements to Applications, Main-Group Elements, Including Noble Gases, Vol. 1* (Ed.: T. Chivers), Elsevier, Amsterdam, **2013**, p. 681; b) I. Krossing, I. Raabe, *Angew. Chem. Int. Ed.* **2004**, *43*, 2066; *Angew. Chem.* **2004**, *116*, 2116; c) C. Reed, *Acc. Chem. Res.* **1998**, *31*, 133; d) S. H. Strauss, *Chem. Rev.* **1993**, *93*, 927.
- [9] Isolation and characterization of radical cations by using the $\{\text{Al}(\text{OR}_F)_4\}^-$ anion and its derivatives: a) S. Zhang, X. Wang, Y. Su, Y. Qiu, Z. Zhang, X. Wang, *Nat. Commun.* **2014**, *5*, 4127; b) Y. Su, X. Zheng, X. Wang, X. Zhang, Y. Sui, X. Wang, *J. Am. Chem. Soc.* **2014**, *136*, 6251; c) F. Gao, F. Zhu, X. Wang, Y. Xu, X. Wang, J. Zuo, *Inorg. Chem.* **2014**, *53*, 5321; d) X. Pan, X. Chen, T. Li, Y. Li, X. Wang, *J. Am. Chem. Soc.* **2013**, *135*, 3414; e) X. Pan, Y. Su, X. Chen, Y. Zhao, Y. Li, J. Zuo, X. Wang, *J. Am. Chem. Soc.* **2013**, *135*, 5561; f) X. Chen, B. Ma, S. Chen, Y. Li, W. Huang, J. Ma, X. Wang, *Chem. Asian J.* **2013**, *8*, 238; g) X. Chen, X. Wang, Z. Zhou, Y. Li, Y. Sui, J. Ma, X. Wang, P. P. Power, *Angew. Chem. Int. Ed.* **2013**, *52*, 589; *Angew. Chem.* **2013**, *125*, 617; h) X. Chen, B. Ma, X. Wang, S. Yao, L. Ni, Z. Zhou, Y. Li, W. Huang, J. Ma, J. Zuo, X. Wang, *Chem. Eur. J.* **2012**, *18*, 11828; i) Refs. [5b,c].
- [10] X-ray data for $2^{2+} \cdot 2[\text{Al}(\text{OR}_F)_4]^-$ and $3^{2+} \cdot 2[\text{Al}(\text{OR}_F)_4]^-$ are listed in Table S1 (SI). CCDC 1015595 (3^{2+}) and 1015596 (2^{2+}) contain the supplementary crystallographic data for this paper. These data can be obtained free of charge from The Cambridge Crystallographic Data Centre via www.ccdc.cam.ac.uk/data_request/cif.
- [11] The C41–C42 bond (1.430(2) Å) is much longer than the bond of C34–C35 (1.356(3) Å), which is probably caused by recovery of the aromaticity of the peripheral benzene ring of naphthalene.
- [12] a) All calculations were performed using the Gaussian 09 program suite. M. J. Frisch, et al., Gaussian 09 (Revision B.01); Gaussian, Inc.: Wallingford, CT, **2010**. See SI for coordinates and full citation; b) The multireference methods other than TD-DFT more properly describe the electronic configurations of the open-shell singlet state of diradicals. However the computational costs of multireference methods are quite high and it is unfeasible for the current study. Nonetheless, TD-DFT methods have been previously shown to be useful in estimating absorption bands of species with diradical character. For latest references, see: c) M. Li, P. J. Hanway, T. R. Albright, A. H. Winter, D. L. Phillips, *J. Am. Chem. Soc.* **2014**, *136*, 12364; d) Ref. [4e]; e) E. V. Canesi, D. Fazzi, L. Colella, C. Bertarelli, C. Castiglioni, *J. Am. Chem. Soc.* **2012**, *134*, 19070; f) Ref. [5a].
- [13] It is worth noting that the most stable electronic states for 1^{2+} and 2^{2+} are open-shell singlets in the gas phase (Table S2, SI). Such a difference between calculation and experimental observations may be ascribed to the counter ion effect. For example, bis(triphenylamine)dications with arylene/vinylene-conjugated bridges were reported to be closed-shell singlets in the solid state but their open-shell singlets have the lowest energy in the gas phase. S. Zheng, S. Barlow, C. Risko, T. L. Kinnibrugh, V. N. Khurstalev, S. C. Jones, M. Y. Antipin, N. M. Tucker, T. V. Timofeeva, V. Coropceanu, J. Brédas, S. R. Marder, *J. Am. Chem. Soc.* **2006**, *128*, 1812.
- [14] The singlet diradical character (y) may be estimated experimentally from the measured quantities obtained from one- and two-photon absorption spectra as well as from phosphorescence and EPR peaks. K. Kamada, K. Ohta, A. Shimizu, T. Kubo, R. Kishi, H. Takahashi, E. Botek, B. Champagne, M. Nakano, *J. Phys. Chem. Lett.* **2010**, *1*, 937.
- [15] a) Calculated by using the reported X-ray crystal structure at the UBHandHLYP/6-31G(d) level;^[2c] b) Calculations show that 3^{2+} has similar diradical character ($y = 0.85$) to its hydrocarbon analogue with N replaced by C atoms (3^{2+}-CA , $y = 0.89$) with a slightly higher $\Delta E_{\text{S-T}}$ (3^{2+} -1.47 ; 3^{2+}-CA -0.93 kcal mol⁻¹). Attempted optimization of hydrocarbon analogues of 1^{2+} and 2^{2+} at the various levels by using the broken-symmetry method did not converge to open-shell singlets (OS) but to closed-shell singlets instead.
- [16] B. Bleaney, K. D. Bowers, *Proc. R. Soc. London Ser. A* **1952**, *214*, 451.
- [17] Spin contamination errors were corrected by an approximate spin-projection method. Y. Kitagawa, T. Saito, M. Ito, M. Shoji, K. Koizumi, S. Yamanaka, T. Kawakami, M. Okumura, K. Yamaguchi, *Chem. Phys. Lett.* **2007**, *442*, 445.